

Development of an Abrasion Resistant Alloy for the Metal Binder Jet Process

Chris Schade, Tom Murphy, and Kerri Horvay
Hoeganaes Corporation
Cinnaminson, NJ 08077

ABSTRACT

In general, hard materials for tooling and wear resistant applications are very difficult to machine, with the most common forming method being grinding. Utilizing a grinding operation severely limits the shape of the final product which can be achieved. Additive manufacturing (AM), specifically, Metal Binder Jetting (MBJ) allows for intricate shapes to be formed for most alloy materials. This paper highlights the mechanical properties and microstructures of an abrasion resistant alloy category called Ni-Hard. Ni-Hard is a generic name for white cast iron materials alloyed with high chromium and nickel which provide abrasion resistance. The microstructure of Ni-Hard alloys generally consists of carbides within a matrix of martensite-bainite and austenite, the levels of which depend on the chemical composition and the heat treatment. The various heat treatments and their subsequent microstructures along with the hardness and abrasion resistance will be studied in samples produced from the MBJ process.

APPLICATION

For manufacturers of metal powders, AM market can be difficult, as it often involves parts with low volumes and the powder used by a specific technique (i.e., Laser Powder Bed Fusion [LPBF], Laser Powder Blown [LPB] or Metal Binder Jetting [MBJ] typically only utilizes one third of the atomized powder distribution. The result is a poor yield of powder for the powder manufacturer and a higher cost for the end user. Developing new alloys for limited applications and small volume production of parts is also difficult to justify for powder manufacturers as the process requires mechanical properties that need to be adjusted per AM technique, and the print parameters for each AM process must be developed. The stringent dimensional tolerances and surface roughness of parts produced by AM require additional development for the material as well.

One application that minimizes these challenges is that of wear resistance, such as grinding or milling, where the part produced is typically sacrificed in the end use, leading to a constant replacement of the part. Ball mill liners and grinding media, hammers used in hammer mills, pulveriser rings, slurry pump parts, sacrificial liners in piping and oil drill bits are just a few of the industrial applications in which the parts are worn during the process and regularly replaced. In these cases, since the material is being sacrificed, the requirements for surface roughness and dimensional tolerances are less stringent, therefore offering the powder producer the ability to utilize a broader particle size distribution, thereby increasing the powder yield. As stated previously, hard materials for tooling and wear resistant applications are difficult to machine and grinding is typically used to shape the part. Since the abrasion/wear resistance of iron and steel alloys tends to correlate with the carbon content, the alloys utilized typically contain more than one percent carbon. This carbon level leads to the formation of martensite and other transformation products in the structure, which can lead to

cracking if the laser methods of additive manufacturing are utilized (LPBF and LPB). The faster cooling rates in the process lead to residual stresses during the solidification of the part, which can lead to cracking in the microstructure. The high carbon contents are beneficial to the MBJ process as the sintering can occur at temperatures more typical of press-and-sinter applications. Because of the higher carbon content of these alloys, the liquidus temperature of the alloy is lowered and diffusion, which enhances the sintering process, is promoted at lower temperatures than most of the current materials for MBJ (i.e., 316L, 17-4PH, etc.)

INTRODUCTION

Wear of an alloy or metal is considered as the removal of material due to forces which act upon the material from another substance. The contacting substance may be another surface, hard particles, a fluid or other media [1]. Wear is progressive removal of material due to the friction of the contacting substance. In general, the wear resistance is correlated with the hardness. The harder the substance in contact with the piece under study, the greater the wear. Conversely, the harder the subject material, the higher its wear resistance. There are additional factors such as operating temperature, environment, contact pressure and material microstructure that also play a role. Therefore, it is difficult to predict the wear properties by looking at the hardness of the materials in question. Figure 1 shows the various wear mechanisms that can exist in metal systems.

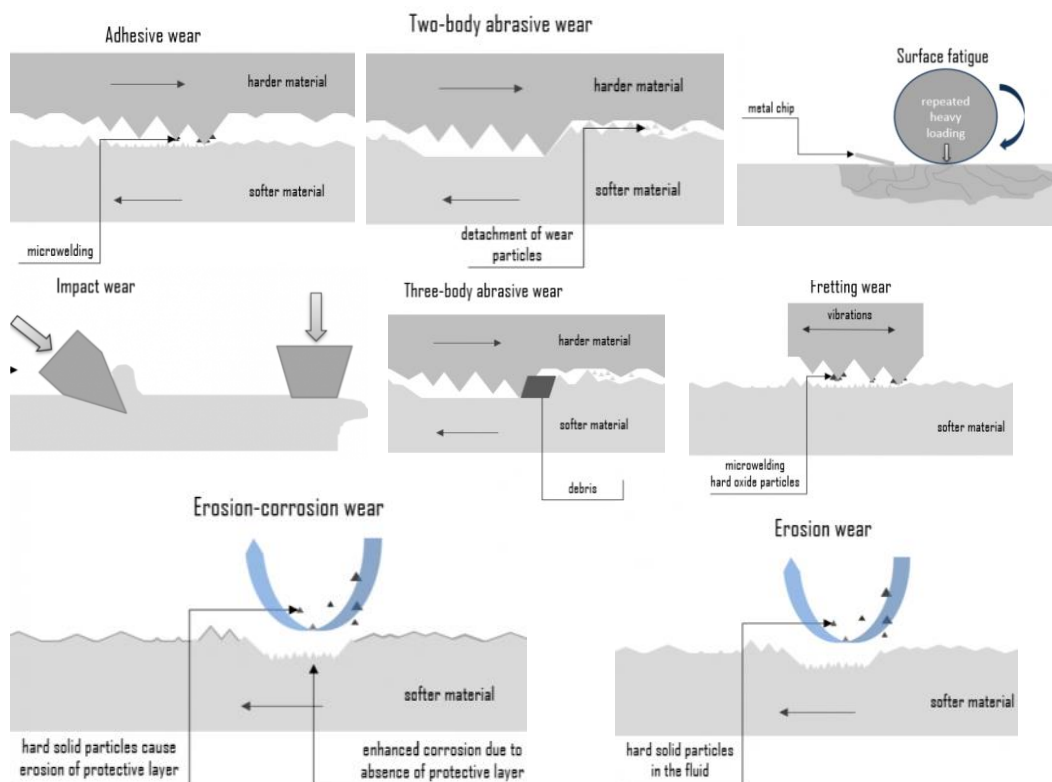


Figure 1: Potential Wear Mechanisms for Materials [2].

Although mechanical properties of an alloy are not the complete descriptor of how they will perform under various wear conditions, they are a useful starting point for defining potential materials for a certain application. Hardness, mechanical strength, and impact strength can help to assess the potential of the material. Specific wear testing that replicates the service conditions of the part is also useful for evaluating materials for specific applications and will be considered.

Additive manufacturing of wear resistant materials is a valuable tool as small prototypes can be made without large costs. These prototypes can be placed in service to collect data on the performance of both the material and design of the part. This can be done without incurring large costs due to molds or machining of extremely hard materials. The design features of AM lend itself to creating parts that could not be produced simply by grinding the shape from a block of metal. Therefore, there is significant potential in utilizing additive manufacturing for producing serial parts for industrial use [3].

BACKGROUND

White cast irons are commonly used in abrasion resistant applications and are covered according to ASTM A532-93 [4]. Ni-Hard, is so named because of the use of nickel in the composition and the high carbon content which leads to high hardness levels. It is a generic name for white cast irons alloyed with carbon, chromium and nickel that provide high hardness and excellent resistance to abrasion. Table I shows the recognized chemical compositions of the Ni-Hard grades as covered by ASTM A532-93 [5]. The grades can be broken down into two categories: Ni-Hard 1 and 2 with nominally 4 wt.% nickel and 2 wt.% chromium, having two levels of carbon, 3.3 and 2.6 wt.% and Ni-Hard 4 with nominally 5 wt.% nickel, 9 wt.% chromium, and 2 wt.% silicon as well as 3 wt.% carbon. The microstructure of the Ni-Hard alloys consists of various carbides and a matrix of martensite with potentially some bainite and austenite depending on the heat treatment process. To better understand the formation of the microstructure and mechanical properties (mainly hardness), it is useful to examine the role of the individual alloying elements.

Table I: Chemical compositions of the Ni-Hard grades per ASTM A532-93. Chemical composition shown in weight percent [4].

Grade	ASTM A532	C	Ni	Cr	Si	Mn	Mo	S	P
Ni-Hard 1	Class 1, Type A	2.8-3.6	3.3-5.0	1.4-4.0	0.80	2.00	1.00	0.15	0.30
Ni-Hard 2	Class 1, Type B	2.4-3.0	3.3-5.0	1.4-4.0	0.80	2.00	1.00	0.15	0.30
Ni-Hard 4	Class 1, Type D	2.5-3.6	4.5-7.0	7.0-11.0	2.00	2.00	1.50	0.15	0.10

Note: Single values are maximums.

Carbon- The carbon content determines the amounts of carbide and the hardness of the matrix phase martensite or mixtures of martensite-bainite and austenite. When comparing the Ni-Hard 1 and Ni-Hard 2 alloys, the higher carbon content in the Ni-Hard 1 alloy leads to a higher level of carbides (of the form M_3C plates) than the Ni-Hard 2. Lower carbon levels generally lead to an alloy with lower hardness but better impact resistance and toughness. Due to the wide range of carbon levels within each alloy designation, the properties can be varied by adjusting the carbon level within the specification range.

In the Ni-Hard 4 alloy, due to the higher levels of chromium, nickel, silicon and carbon, the alloy forms a eutectic or slightly hypoeutectic alloy and the carbide structure is rod-like $(Cr,Fe)_7C_3$, the volume of which is less than in Ni-Hard 1 and 2. Both the lower volume of carbide and the rod-like carbide morphology lead the alloy to have a lower abrasion resistance than the Ni-Hard 1 and 2 but a higher resistance to impact. In castings, the matrix phase in Ni-Hard alloys is austenite which can be transformed to different levels of martensite and/or bainite and additional carbides by various heat treatments. These various combinations lead to a range of hardness, fracture resistance and wear resistance that can be achieved.

Nickel- Nickel is an austenite former and is added to ensure that a martensite/bainite matrix, without pearlite, is formed. It also increases the alloy hardenability. The level of nickel increases with increasing levels of chromium (a ferrite stabilizer), however, too much nickel will lead to increased formation of retained austenite. The austenite, if present in significant amounts, will lower the hardness and increased abrasion can occur due to the lower hardness of the matrix. In the Ni-Hard 4 alloys, the nickel also assists in the formation of the $(Cr,Fe)_7C_3$ carbides.

Chromium- In Ni-Hard 1 and 2, chromium is added to compensate for the graphitizing effect of nickel in the cast iron. If graphite precipitates form, they act as soft spots and reduce hardness and abrasion resistance. In general, the chromium is concentrated in the carbides and increases hardness. In Ni-Hard 4, the high chromium content (typically 8-10 wt.%) is also required to form the $(Cr,Fe)_7C_3$ carbides, instead of the $(Cr,Fe)_3C$ carbides which have lower hardness. Finally, the chromium that is not tied up as carbides increases the hardenability of the matrix phase.

Silicon- In general, silicon is a graphitizer in cast irons and should be kept as low as possible, but also it is added to assist in the casting process (for fluidity). As stated previously, the formation of graphite is to be avoided as it reduces the hardness and abrasion resistance. In the Ni-Hard 4, the silicon assists in forming the rod-like $(Cr,Fe)_7C_3$ carbides and lower silicon levels will form mixed carbide morphologies which may lead to lower toughness and abrasion resistance. Silicon also increases the hardenability of the matrix and promotes the transformation from austenite to martensite. In the Ni-Hard 4 alloy, the graphitizing effect of silicon can be counteracted by increased levels of chromium.

Molybdenum- Molybdenum can be added in small amounts to increase the hardenability of all three alloys. In cases where the carbon (and nickel) are added to the higher levels, molybdenum can be added to prevent excessive amounts of retained austenite. Molybdenum also can be present in the carbide phase and has been documented to prevent carbide coarsening during heat treatment [6].

Manganese- Manganese increases hardenability of the matrix phase but also promotes the formation of retained austenite and, therefore, is generally kept at a level of 0.50 wt.% or lower.

Sulfur and Phosphorus- Both elements are considered detrimental and reduce toughness. Additionally, sulfur can combine with manganese to form soft manganese-sulfides which reduce the abrasion resistance of the material.

Niobium, Titanium, Tungsten and Vanadium- These elements are used in special grades of Ni-Hard and form fine carbide precipitates. Recent studies have used these elements to increase the precipitation rate and form a fine dispersion of carbides which improve the abrasion resistance of the alloys to which they are added [7-14]. The improved abrasion resistance occurs without the reduction in impact properties. The carbon level in the alloy must be balanced with the addition of the elements to ensure there is enough to form the maximum level of carbides.

EXPERIMENTAL PROCEDURE

Melting

The influence of the alloying elements discussed in the previous section was used as the basis to manufacture experimental powders to determine how the Ni-Hard grades could be utilized in the MBJ process. Compared with the chemical compositions of the cast versions shown in Table I, the only modification for the chemical composition of the water atomized powder was to keep the manganese to a minimum in order to keep the oxygen low in the powder (Table II). It is known from previous work that higher manganese levels can lead to high oxygen content in the water atomized powder [15]. Both Ni-Hard 1 and Ni-Hard 4 alloy compositions were manufactured for testing with vanadium additions, as the recent work has shown improvements to the wear resistance over the standard Ni-Hard grades without vanadium [7,16]. Two different vanadium levels (high and low) were chosen for the Ni-Hard 4 composition. Since the materials were being melted in an induction furnace with no protective atmosphere, vanadium was chosen over titanium since the latter would have oxidized and led to clogging of the molten metal delivery tube to the atomizer. Tungsten was avoided due to its density and high melting point, both of which increase the probability that it is left unmelted at the bottom of the furnace. Niobium was also not chosen, since the MBJ process with sintering was to be utilized. Niobium carbides require higher temperatures to go into solution and the carbides formed from cooling during the sintering process would coarsen during the heat treatment step and, therefore, not be optimal for hardness and wear resistance.

Table II: Chemical composition of Ni-Hard alloys produced by induction air melting. Chemical composition shown in weight percent.

Material	Si	P	V	Cr	Mn	Ni	Mo	Carbon	Sulfur	Oxygen	Nitrogen
Ni-Hard 1	0.67	0.08	2.79	3.51	0.26	4.67	1.02	3.25	0.033	0.22	0.08
Ni-Hard 4 Low V	1.59	0.04	0.89	8.91	0.14	5.60	1.08	2.89	0.015	0.39	0.02
Ni-Hard 4 High V	1.86	0.08	2.85	9.12	0.21	6.26	1.05	2.90	0.034	0.29	0.03

Atomizing

The powders were water atomized using two different water pressures. The two higher vanadium alloys (Ni-Hard 1 and 4) were atomized at 19 MPa, while the Ni-Hard 4 with low vanadium was atomized at 48 MPa. Typical powder sizes used in MBJ are < 25 μm . In order to maximize yield for this requirement, high atomizing pressures are typically utilized. The two alloys atomized at the lower pressure were done intentionally so that the distribution could be processed for both MBJ and LPBF; the latter normally utilizes a 20-63 μm particle size distribution of the powder. Atomizing at the lower pressure allowed both particle size distributions to be produced from a single melt/atomizing run. The distribution for LPBF will be studied in future work.

The particle size and physical attributes of the powder are shown in Table III. After atomizing and drying, the powders were screened. The powders atomized at 19 MPa were screened minus 53 μm (with the oversize powder being utilized for work with LPBF) and the powder (Ni-Hard 4 Low V) atomized at 48 MPa was screened minus 38 μm , which yielded a particle size distribution typically utilized in MBJ.

Table III: Powder properties of air melted and water atomized Ni-Hard alloys.

	Apparent Density	Tap Density	Hall Flow	d ₁₀	d ₅₀	d ₉₀
Material	g/cm ³	g/cm ³	(Secs)	Micrometers	Micrometers	Micrometers
Ni-Hard 1	3.7	4.8	34.9	12.8	27.9	51.1
Ni-Hard 4 Low V	2.9	3.9	NF	5.6	14.1	28.6
Ni-Hard 4 High V	3.5	4.4	45.5	11.9	27.3	50.9

Sample	Mean Circularity	Mean Length (micrometers)	% Porosity	% Particles with Porosity
Ni-Hard 1	0.73	20.84	0.42	3.93
Ni-Hard 4 High V	0.72	19.95	0.50	3.36
Ni-Hard 4 Low V	0.65	13.54	0.84	4.22

Water atomization typically leads to irregular particles compared with gas atomized powders due to the rapid quenching and high impact momentum of the water jet. In addition, the Ni-Hard 4 with low vanadium, which was atomized at the higher water pressure, has a lower apparent density and tap density than the two powders atomized at the lower pressure. Powder particles were cross-sectioned and polished and image analysis was performed to measure the shape of the particles and the level of porosity in the interior of the particles. These results are also shown in Table III. The Ni-Hard-4 Low V, which was atomized at the higher water pressure, had a more irregular shape (mean circularity much less than 1) and an increased level of porosity compared to the other two powders.

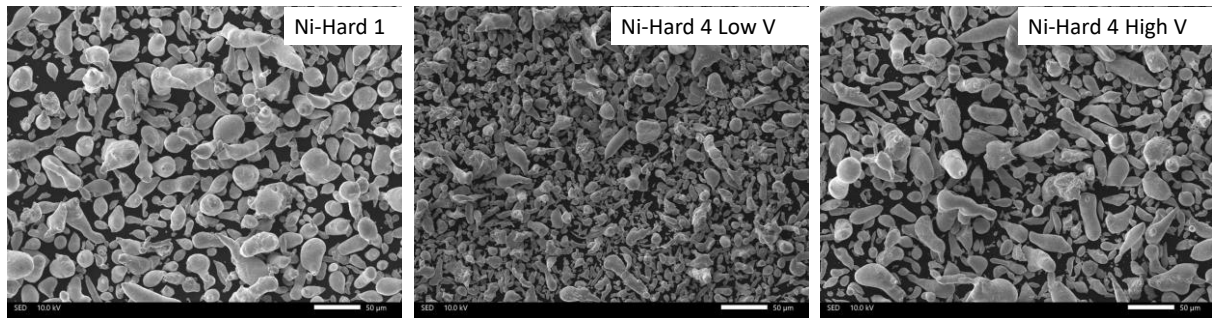


Figure 2: Scanning Electron Microscopy (SEM) images of the water atomized powders.

SEM images of the powders are shown in Figure 2. All three powders are similar in shape, with elongated particles typically seen in water atomized powders of high carbon content. The increased carbon content lowers the viscosity and leads to the more elongated particles with smooth powder surfaces. The finer particle size of the high-water pressure atomized Ni-Hard 4 Low V is evident but the shape and texture of the powder is similar to the other two alloys atomized at lower water pressure.

Printing

The powders were printed on an ExOne Innovent Plus with a solvent binder with layer thickness between 50-75 µm. All test specimens were printed in the X-Y plane with the Z

direction being the specimen thickness dimension. After depowdering, the specimens were cured in air at 200 °C for 4 hours.

Green density and green strength for the three alloys are shown in Table IV. Since the water atomized powders have a low apparent density compared to gas atomized powders, the density after printing is somewhat lower than gas atomized powders which typically run 4.0 g/cm³ or lower. However, the green strength of the water atomized powders is similar to gas atomized powders due to the irregular shape of the powder which increases the mechanical interlocking between particles.

Table IV: Green and sintered properties of TRS (transverse rupture bars)

	Green Density	Green Strength	First Liquid Temp.	Sintering Temp.	Sintered Porosity	R _a	R _z
Material	g/cm ³	MPa	°C	°C	(%)	Micrometers	Micrometers
Ni-Hard 1	3.61	2.8	1126	1120	(0.16-0.18)	3.94	23.07
Ni-Hard 4 Low V	3.93	2.5	1164	1138	(0.19-0.25)	1.29	8.36
Ni-Hard 4 High V	3.03	2.8	1178	1177	(0.08-0.20)	4.05	23.80

Sintering

All test pieces were sintered in an Abbott continuous-belt furnace at temperatures ranging from 1138 °C (2080 °F) to 1177 °C (2150 °F) for 45 min in 95 vol.% nitrogen and 5 vol.% hydrogen.

Due to the high alloy content, specifically carbon, the melting points of the alloys are relatively low compared to low alloy steels. Therefore, the selection of the sintering temperature must take into account that a high volume fraction of liquid would cause parts to slump or have dimensional issues. Table IV shows the temperature at which the first liquid starts to form in each of the alloys based on calculations made with a thermodynamic software (Thermo-Calc). Since the Ni-Hard 1 has the highest carbon level, and since carbon has the biggest influence on melting point, the first liquid forms at around 1126 °C. For the Ni-Hard 4 alloys, the temperature at which the first amount of liquid forms is higher due to the lower carbon levels (the Ni-Hard 4 Low V forms the first liquid at 1164 °C and the Ni-Hard 4 High V at 1178 °C). Based on these calculated values, sintering trials were performed at various temperatures to optimize the density of the sintered specimens. Table IV shows the selected sintering temperature for the three alloys along with the corresponding porosities measured by image analysis. All three alloys had porosity levels < 0.5 vol.%.

Another output from the sintering experiment was the surface roughness. Surface roughness of the sintered bars was measured using Mitutoyo SJ-210 surface roughness tester. The tester traces the surfaces of the specimen and calculates the surface roughness based on a set of known roughness standards. Two parameters that were used in this study to quantify the roughness of the bars are as follows:

R_a which is the arithmetic mean of the absolute values of the evaluation profile deviations from the mean line. It represents the calculated average between the peaks and valleys on a surface.

R_z where the evaluation profile is divided into segments and for each segment the highest point and lowest point from the mean line is calculated. The average of these sums is R_z. It is

the difference between the highest peak and the lowest valley within the sampling of maximum roughness.

For both R_a and R_z , the lower the magnitude of the measurement, the lower the surface roughness. It can be seen in Table IV that the finer particle size of the Ni-Hard 4 Low V led to a lower surface roughness, while the other two alloys, with very similar particle size distributions, were very consistent to each other. The values also compare favorably to 316L printed in the same manner ($R_a = 5.5 \mu\text{m}$ and $R_z = 33.5 \mu\text{m}$).

One final consideration for the sintering of water atomized powders is the oxygen content. Although the initial oxygen content in the powder from water atomization is significantly higher than gas atomized powders, when the part is sintered, the oxygen is reduced by the hydrogen in the sintering atmosphere (5 vol.%) to levels typically found in parts made from gas atomized powders. Oxygen values for both gas and water atomized Ni-Hard alloys ranged from 200-350 ppm after sintering.

Heat Treatments

Heat treatments were performed in a batch-box furnace at 793 °C (1460 °F) for various times in a nitrogen atmosphere followed by air cooling unless otherwise noted.

Hardness is usually the one property that is used to evaluate the performance of the Ni-Hard castings, since it is very difficult to machine suitable test samples (i.e. tensile and Charpy impact bars) from the materials as they are hard and brittle. In addition, most standards covering this alloy class only specify hardness for the fact that the other properties do not represent the performance of the material in service. For this, wear testing is a more appropriate method for evaluation, and was conducted as part of this study. Apparent hardness measurements were made on the specimens, in accordance with MPIF Standard 43 [17].

Wear Testing

Wear testing to investigate the effect of scratching abrasion on each alloy was completed according to ASTM G65 Procedure A, "Standard Test Method for Measuring Abrasion Using the Dry Sand/Rubber Wheel Apparatus". This type of wear depends upon factors including the abrasive particle size, shape, hardness, frequency of contact, etc. [18]. The test can provide a relative ranking of materials tested, but cannot predict the exact wear resistance in a specific environment. The mass of each sample was recorded before and after the test. The hardness of the abrasion samples was also measured. A diagram of the test is shown in Figure 3. A test specimen is pressed against a rotating wheel while an abrasive sand is flowed between the specimen and the wheel. Abrasion test samples (76 mm x 25 mm x 13 mm) of each alloy were printed horizontally. The specimens were printed as oversize blocks and then machined down to size. They were cured, sintered and then heat treated before testing. The flow rate of sand between the neoprene rubber wheel and specimen was at a rate of 300-400 g/min with a test load of 133 N. The samples were subjected to 6000 cycles for a 30 minute duration.

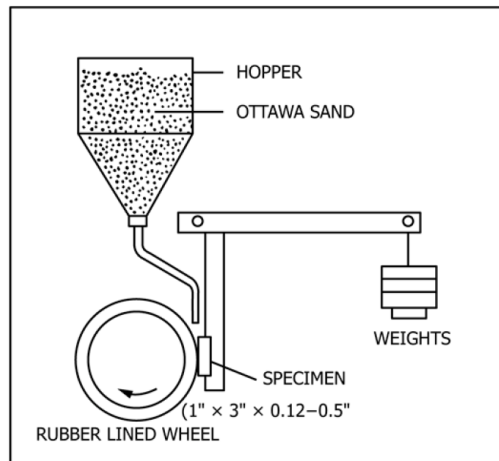


Figure 3: Schematic of Abrasion Testing Apparatus per ASTM G65.

Metallography

Metallographic specimens of all the test materials were examined by optical microscopy in the polished and etched conditions. Etched specimens were used for microindentation hardness testing as per MPIF Standard 51 [17].

RESULTS AND DISCUSSION

Heat Treatments

Ni-Hard alloys are usually given one of four heat treatments [5]:

1. A stress relief at low temperatures 225-275 °C (437-527 °F) for improved toughness.
2. A two-step heat treatment, 450 °C (840 °F) followed by 275 °C (495 °F) for improved impact fatigue resistance.
3. Cryogenic Heat Treatment
4. Heating to 750-850 °C (1350-1560 °F) and holding for various times, followed by a slow cool with optional tempering. This is considered a hardening heat treatment.

Since the MBJ process requires sintering, the cooling at the end of the sintering cycle gives a different microstructure than the castings for which the alloy was developed. This needs to be considered when selecting the appropriate heat treatment for comparison to the wrought material.

The stress relief treatments at low temperatures are used to temper the martensite, provide isothermal formation of bainite and to transform any retained austenite to martensite. In general, these treatments do not lead to a significant increase in hardness and the magnitude of the change depends on the levels of martensite and retained austenite in the starting structure.

The two-step heat treatment involves heating in austenite to promote secondary carbide precipitation, which occurs due to the diffusion of carbon from the austenite to the carbide. Upon air cooling, any remaining austenite will transform to martensite. During the second stage heating at 275 °C (495 °F), this newly formed martensite will be tempered and any martensite that was remaining will be more heavily tempered, and a loss of hardness will

occur. This heat treatment is not utilized for improvements in abrasion resistance but for applications where increased fatigue resistance is required such as grinding media and mill liners.

Utilizing cryogenic treatment can be accomplished by utilizing liquid nitrogen where the sub-zero temperatures allow for any retained austenite in the structure to transform to martensite. In castings, the same hardness values can be obtained by optimizing the chemical composition of the alloy so it is not commonly practiced, but for complex shapes, where heat treatment is complicated by the shape of the part, it may be of value. This may be beneficial if the MBJ part being produced is complex in shape but must have the same hardness throughout the part.

The final heat treatment, hardening, is accomplished by first heating into the austenite range and holding, allowing the carbon to diffuse from the austenite and assisting the formation of secondary carbides (primary carbides were formed during the sintering process). During air cooling to room temperature, the remaining austenite transforms to martensite, while additional carbides are also formed. The martensite also undergoes a certain amount of tempering during the cooling process.

Since the applications being investigated (see case study section) involved maximizing the abrasion resistance, all three of the experimental materials were given the hardening heat treatment. Transverse rupture strength (TRS) bars for hardness measurements (Rockwell C-HRC) were heated to 709 °C (1460 °F) under nitrogen for various times and then air cooled. The results are shown in Figure 4.

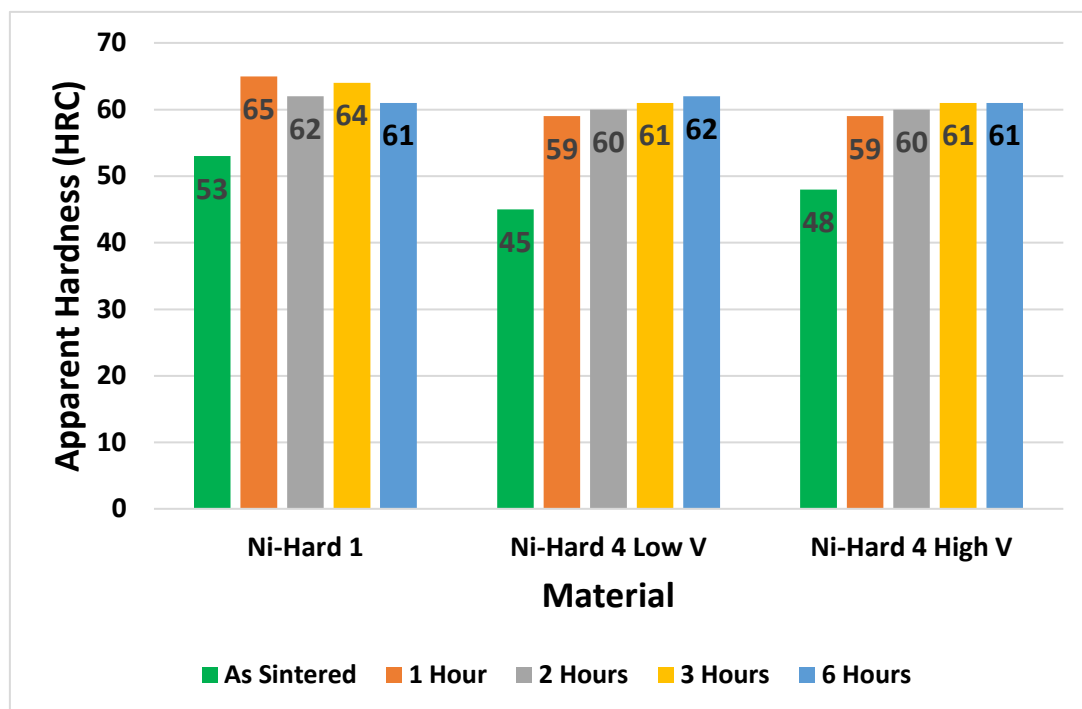


Figure 4: Hardness of experimental alloys- as sintered versus 1,2,3 and 6 hours at 793 °C (1460 °F).

The hardness of all three alloys significantly increased from the sintered state to the heat-treated condition (for all holding times) with the Ni-Hard 4 Low V and Ni-Hard 4 High V both achieving an HRC value of 59 after one hour at 793 °C (1460 °F). Since the grain size of the castings is so much larger than the atomized/sintered powder, the time at temperature to achieve maximum hardness is lower for the MBJ process versus cast materials. The apparent

hardness of the Ni-Hard 1 reached a higher maximum hardness of HRC 65 after 1 hour at temperature, which is expected as this alloy is designed for maximum abrasion resistance.

The apparent hardness is not the only indicator of the wear resistance of a material. The volume fraction of the harder phase (carbide) and the hardness of that phase are the primary indicators of wear resistance. Table V shows the percentage of phases and the micro-indentation hardness of those phases for each of the grades. While the Ni-Hard 1 had the highest apparent hardness, the micro-indentation hardness of the carbide phase was the lowest of the three alloys (~1031-1115 HV). The volume percentage of the carbide phase was on average the highest. The Ni-Hard 4 with low vanadium, which had the lowest apparent hardness, had the highest average hardness of the carbide phase in the heat-treated condition (~1551-1879 HV), with only a slightly lower volume fraction of the carbide phase. The apparent hardness (HRC) of the Ni-Hard 4 with high vanadium was at a similar level to the Ni-Hard 4 with Low V, but the micro-indentation hardness of the carbide phase was much lower. The hardness of the secondary phase, primarily martensite in all three grades, increased in order from Ni-Hard 4 Low V to Ni-Hard 4 High V to Ni-Hard 1. In general, the peak hardness for all three alloys was found to occur with a heat treatment at 709 °C (1460 °F) for 1 to 2 hrs.

Table V: Micro-indentation hardness (MIH) and volume fraction of phases present in Ni-Hard Alloys

Ni-Hard 1	Apparent Hardness (HRC)	Carbide Phase (vol.%)	Carbide MIH (HV_{100gf})	Secondary Phase (vol.%)	Secondary Phase MIH (HV_{100gf})
As Sintered	53	34.6	1064	65.4	469
1 Hour	65	33.5	1031	66.5	780
2 Hours	62	38.3	1115	61.7	873
3 Hours	64	37.1	1040	62.9	814
6 Hours	61	37.1	1042	62.9	889
Ni-Hard 4-Low V	Apparent Hardness (HRC)	Carbide Phase (vol.%)	Carbide MIH (HV_{25gf})	Secondary Phase (vol.%)	Secondary Phase MIH (HV_{100gf})
As Sintered	45	24.6	1120	75.4	439
1 Hour	59	34.6	1879	65.4	609
2 Hours	60	32.5	1767	67.5	606
3 Hours	61	29.6	1551	70.4	745
6 Hours	62	29	1682	71.0	719
Ni-Hard 4 High-V	Apparent Hardness (HRC)	Carbide Phase (vol.%)	Carbide MIH (HV_{50gf})	Secondary Phase (vol.%)	Secondary Phase MIH (HV_{50gf})
As Sintered	48	27.7	1161	72.3	474
1 Hour	59	30.4	1214	69.6	737
2 Hours	60	38.1	1220	61.9	725
3 Hours	61	35.8	1157	64.2	703
6 Hours	61	24.4	1182	75.6	705

The microstructures from samples heat treated for 2 hours at both low and high magnification are shown in Figure 5. The microstructure consists of carbides (lighter phase) with a mixture of martensite/bainite as the matrix phase (the darker phase) with a small amount of retained austenite. The carbide network in the Ni-Hard 1 alloy is blocky and coarse compared to the structure of the other two materials, which are finer and more evenly distributed. SEM analysis along with Energy Dispersive Spectroscopy (EDS) of the carbide phase shows that

the carbides consist of chromium carbides and chromium-vanadium carbides (with both carbides containing molybdenum and silicon). The hardness range for the carbides was 800-1200 HV for the chromium carbides and 1550-2200 HV for the chromium-vanadium carbides. The results in Table V do not distinguish between these carbides and are an overall average.

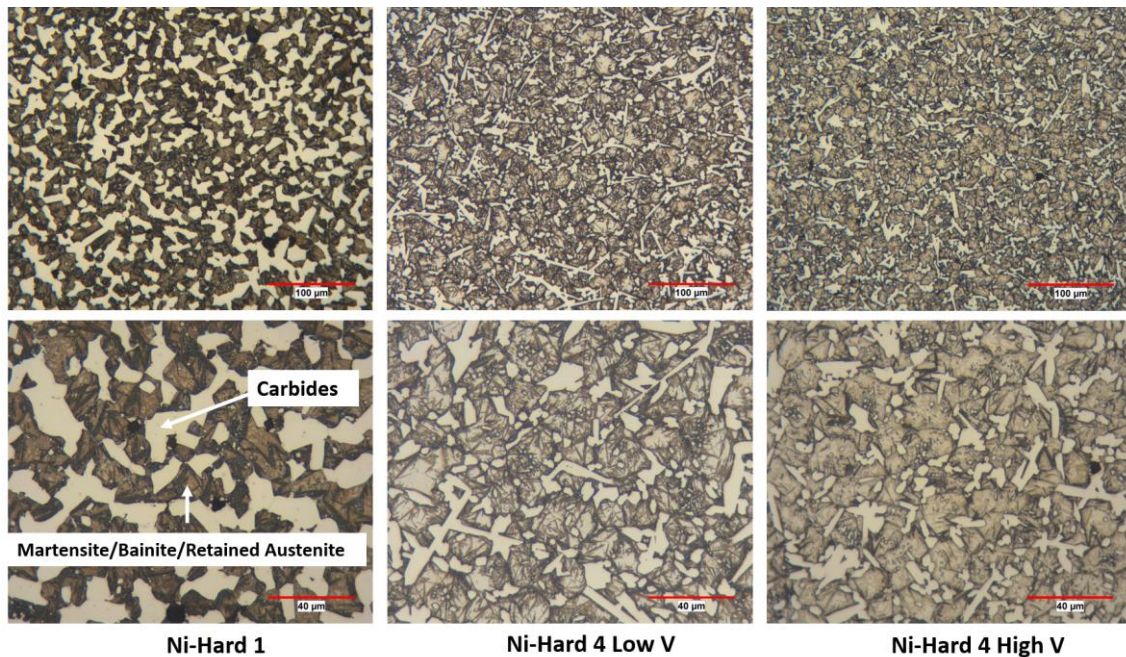


Figure 5: Microstructures of the Ni-Hard alloys shown at both low (top) and high magnifications (bottom).

Wear Resistance

It is generally accepted that the harder the material, the better the wear resistance a material will have. In reviewing Table V, the Ni-Hard 4 Low V had the highest hardness in the carbide phase with only a slightly lower hardness of the matrix phase compared with the other alloys. The volume fraction of the second phase is also close to the other two alloys. Assuming that the abrasive wear resistance of the alloy will be related to the hardness and volume fraction of the second phase, the Ni-Hard 4 Low V was chosen to perform the wear testing as set out in ASTM G65 Procedure A. The lower carbide volume and rod-shaped carbides result in higher impact resistance of Ni-Hard 4 then compared with Ni-Hard 1. As later discussed in the case study, the specific application for which this study was undertaken was for a hammer in a grinding apparatus which needs to have a certain level of impact toughness. For this reason, the Ni-Hard 4 Low V was chosen for the examination of wear resistance by performing testing according to ASTM G65 Procedure A.

Based on the results from Table V, samples for the wear test (as outlined in the Experimental Procedure Section) were prepared by printing-curing-sintering and heat treating. Samples were evaluated that covered a range of the hardness of the carbides, and the weight loss of the samples were plotted versus the hardness of the carbides as shown in Figure 6. As expected, the weight loss of the block samples decreased as the micro-indentation hardness of the carbides increased. A strong correlation existed between the two variables and gave confidence to proceed with the Ni-Hard 4 Low V for the case study.

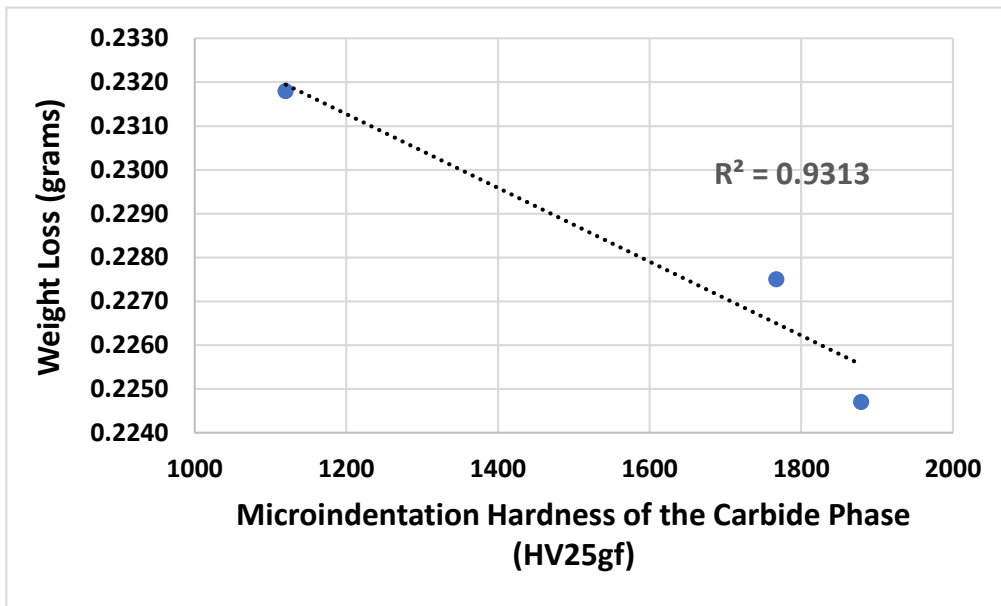


Figure 6: Weight loss as a function of microindentation hardness of the carbide phase.

Procedure A of ASTM G65-16 is described as test to rank metallic materials on a wide range of scratching abrasion resistance from low to extremely high. Since it is a standardized test with controlled parameters, it is particularly useful in ranking materials against each other. The test parameters for the Ni-Hard material were chosen (as outlined in the experimental procedure) so that the results of this study could be compared directly to relevant materials tested in ASTM G65-16, which were validated for precision by several laboratories. The results of the Ni-Hard 4 Low V are compared to these materials in Table VI.

The mass loss or volume loss, as presented in Table VI, represent the abrasion loss during the test and, therefore, the lower the loss (either mass or volume), the better the abrasion resistance. In examining the ranking of materials, the Ni-Hard Low V alloy performed significantly better than both the H13 and D2 tool steels which also have been successfully printed by MBJ. However, the tooling in which these alloys are used does not require any fracture or impact toughness requirements and, hence, these materials are brittle. Also shown is an abrasive resistant low alloy steel, AR600 (typical commercial Brinell hardness = 600), manufactured in plate form for applications such as buckets for front end loaders, linings of rail cars, and grinding equipment linings. The material has better impact resistance than the tool steels but lower hardness. Finally, there is a carbide material (composition unspecified) listed which has high abrasion resistance but can be assumed to be very brittle. If you consider that the Ni-Hard 4 Low V alloy only has approximately 30% volume fraction of carbide, the wear resistance is quite good when compared to the carbide listed in Table VI.

Table VI: Materials evaluated by Procedure A of ASTM G65-16 Abrasion Wear Test.

Material	Mass Loss (grams)	Volume Loss (mm ³)	Source
AR600 (Tempered)	1.80	236.0	Reference [19]
H13 Tool Steel	0.42	55.0	ASTM G65-16
D2 Tool Steel	0.33	41.8	ASTM G65-16
Ni-Hard 4 Low V (2 hrs)	0.23	29.9	This Study
Carbide	0.11	9.6	ASTM G65-16

CASE STUDY

Although unproven, AM techniques for making wear resistant parts should have a distinct advantage over current machining processes. Because the materials necessary for good wear resistance have high hardness, the machining of parts, other than simple geometries, is difficult. In these cases, the only viable method for shaping the part is grinding, which limits the design capability of the part which leads to poor material yield. AM, particularly MBJ, would then seem to have an advantage in this regard as the design freedom can be increased with low material waste.

Based on the work done in this study, it appeared the hardness and wear resistance of the Ni-Hard alloys produced by MBJ would make the materials and the process suitable for industrial use. Therefore, a case study in which parts were made and placed in service was undertaken. Figure 7 shows a typical mill for grinding material. Material is fed into the mill while hammers are rotating at high revolutions per minute (RPM). The material is shattered and forced through a mesh screen with different hole sizes corresponding to the final particle size targeted. The material then exits the mill and is collected in a container. These types of mills are used to grind a variety of products, including ferro-alloys for the steel industry, hard magnet alloys and metal hydrides.

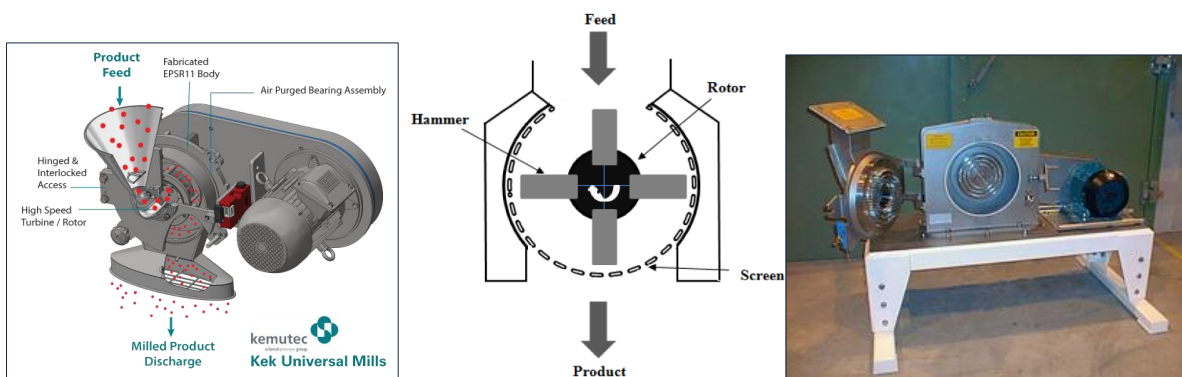


Figure 7: Typical hammer mill configuration for grinding materials.

The lifetime of the hammers utilized in the mill is critical as the productivity of the mill is reduced if frequent hammer changes are required. Typically, the hammers are ground or shaped from abrasion-resistant plate steels (AR400- Brinell Hardness = 400, HRC ~ 43). For the case study, the hammers shown in Figure 8 were printed by MBJ from the Ni-Hard 4 Low V alloy. Grinding trials were performed and wear and lifetime of the AM printed parts were quantified. The material that was ground was a metal alloy comprised of samarium-cobalt with a hardness of HV = 600-650. Four MBJ hammers were installed in each one of the four quadrants of the rotating cage shown in Figure 8. The rest of the hammer positions were filled with standard hammers machined from an abrasive-resistant plate AR400.

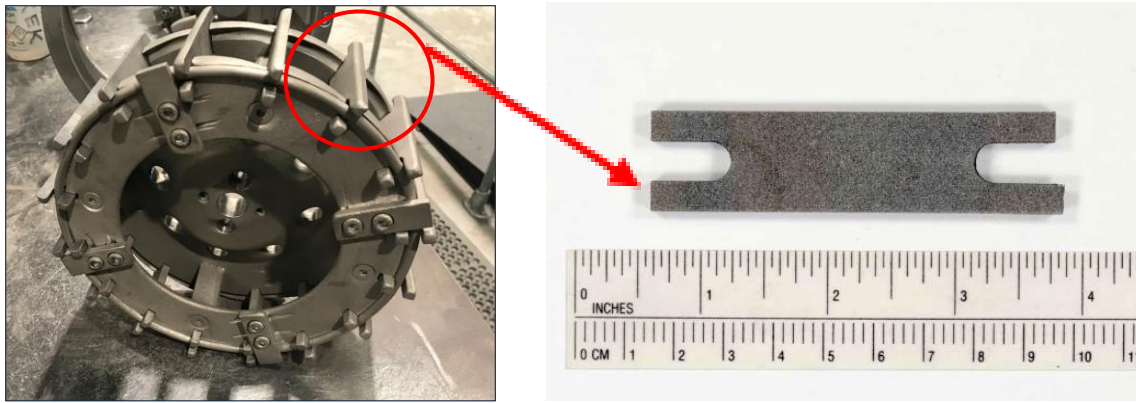


Figure 8: Rotating cage with hammers on the perimeter (left) and hammers (right).

Approximately 1300 kgs of material was processed over a period of four days. During this period, there were frequent starts and stops of the grinding equipment, which allowed for examination of high impact events. Although the family of Ni-Hard 4 alloys were designed to have better impact toughness for applications such as milling, there was still concern for this application, as the rotating cage operates at 3000 RPM and if one of the hammers were to break, considerable damage to the equipment would occur. The multiple starts and stops without failure proved that the material could withstand this high impact force of the application.

Table VII: Wear measurements of hammers used in case study.

	Initial weight [g]	Initial height [mm]	Final weight [g]	Final height [mm]	Change in weight [g]	Change in height [mm]	% Change in Weight
AR400 Hammer	64.34	5.82	61.46	5.70	-2.88	-0.12	-4.48
MBJ Hammer 1	63.32	6.15	63.43	5.99	0.11	-0.16	0.17
MBJ Hammer 3	57.67	5.53	57.78	5.54	0.11	0.01	0.19
MBJ Hammer 4	63.89	6.16	63.97	6.12	0.08	-0.04	0.13
MBJ Hammer 6	63.91	6.26	64.03	6.15	0.12	-0.11	0.19

The wear resistance of the hammers was measured using two parameters before and after processing (Table VII) the 1300 kgs of Sm-Co alloy: the weight of the hammer and the height of the hammer (which included the surface that was impacted by the material). The MBJ Ni Hard-4 Low V hammers showed no significant change in weight, while the standard hammer lost ~4.5% of the starting mass. Measurements of the thickness and the height of the hammer showed very little change dimensionally, however, upon examination of the hammers under a stereoscope, it was determined that most of the wear occurred on the corners of the hammer (Figure 9) and were not accurately represented by these measurements. The stereoscope images reveal much heavier wear on the corners of the AR400 hammers versus the Ni-Hard 4 Low V MBJ hammers.

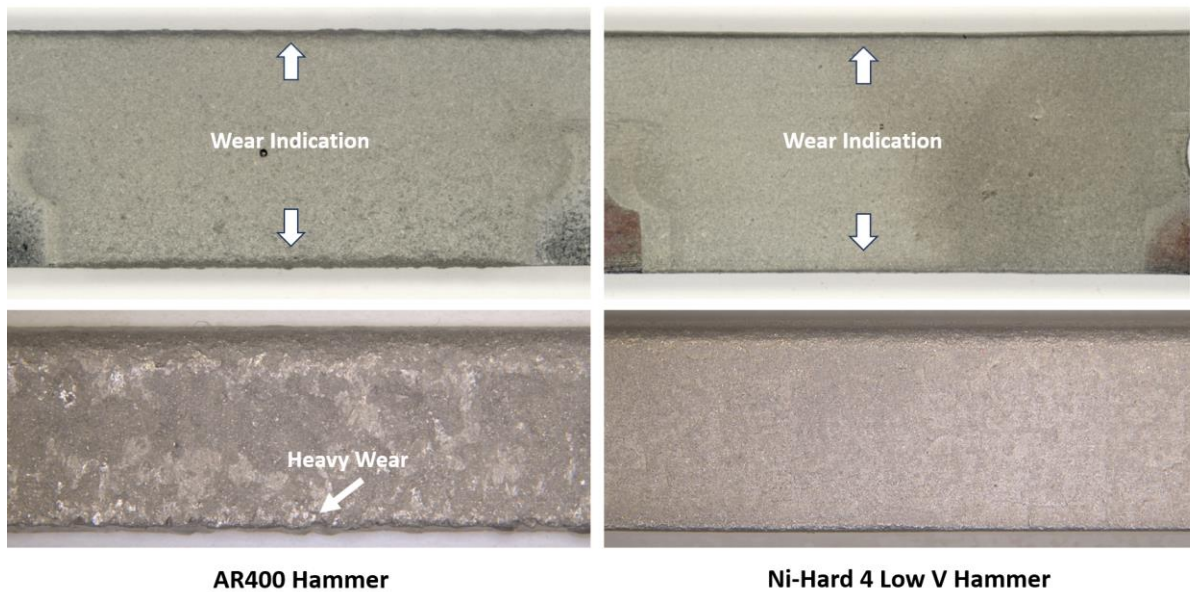


Figure 9: Macro pictures showing wear on standard hammers (AR400) versus Ni-Hard 4 Low V hammers produced by MBJ.

Cross sections of the corners of the two hammers are shown in Figure 10. The unetched section (far left) shows a considerable amount of material was removed from the corner of the AR400 when compared to the MBJ printed hammer. Additionally, the etched microstructure at low magnification (Figure 10b) shows that the material being ground (Sm-Co) has become embedded in the AR400 hammer. Since the hardness of the AR400 hammer is much less than the Sm-Co being ground, the material penetrates the hammer surface and contributes to the wear by being continuously broken off, taking part of the matrix material with it, then redepositing as further grinding takes place. This cycle repeats and leads to the higher weight loss of the AR400 hammer. Since the carbide phase in the Ni-Hard 4 hammers is much harder than the Sm-Co (HV = 1500 versus HV = 650), there is little of the Sm-Co embedded in the MBJ printed hammers, hence, the lower weight loss during the trial period. The effect of the impact of the Sm-Co can be seen in Figure 10c. There is a visible deformation of the microstructure in the corner of the AR400 hammer, while the Ni-Hard 4 MBJ hammer shows no deformation. The bulk hardness of the AR400 hammer is 35 HRC, which is much softer than the bulk hardness of the Ni-Hard 4 (HRC ~ 60). This increased deformation resistance of the Ni-Hard material should lead to more efficient grinding and longer life since the hammer can maintain the original shape for a greater period.

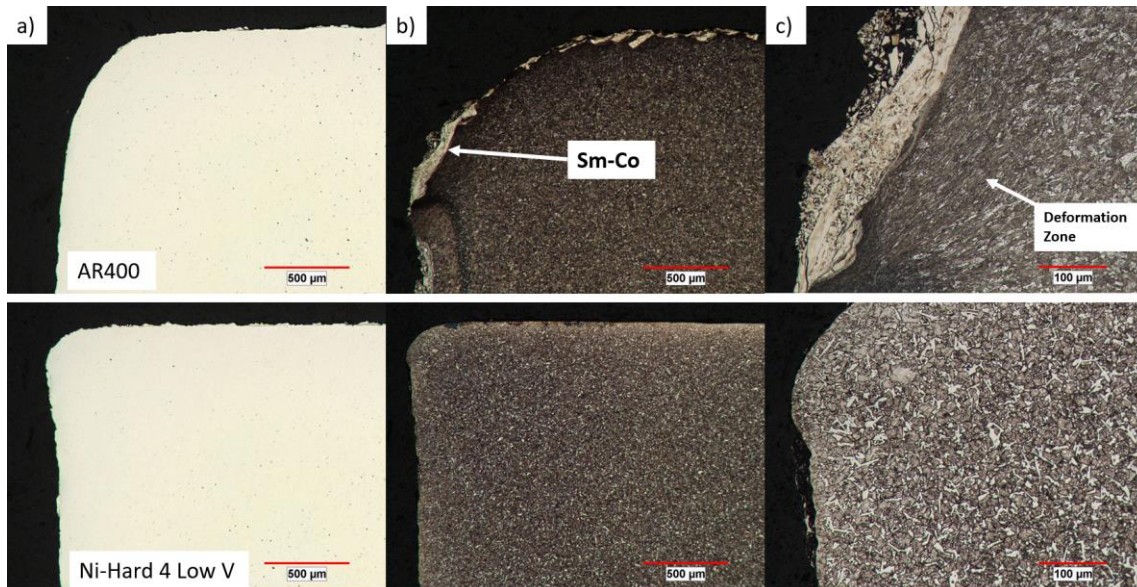


Figure 10: High magnification micrographs of AR400 hammer (top) and Ni-Hard 4 Low V (bottom) showing wear (a and b) and deformation zones in high wear area (c).

CONCLUSIONS

- Ni-Hard Alloy powders produced by water atomization are suitable for the MBJ process in the production of parts.
- The Ni-Hard Alloys are sintered using conventional PM sintering furnaces due to the low sintering temperatures and conventional sintering atmosphere.
- The hardness of the Ni-Hard Alloys can be increased from the as sintered condition by heat treatment and match the cast material hardness values reported in literature.
- The abrasion resistance, as measured by ASTM G65-16, shows that the Ni-Hard Low V produced by MBJ can achieve levels higher than conventional tool steels that are used for mold applications.
- The wear of Ni-Hard 4 Low V, as evaluated by Procedure A of ASTM G65-16 for abrasion wear testing, was significantly improved over low alloy abrasion resistant steels as well as conventional tool steels such as H13 and D2.
- The sintered density of the MBJ Ni-Hard can exceed 99% since the alloys can be sintered close to their liquidus temperature.
- Trials producing hammers for impact mill applications showed that the Ni-Hard 4 Low V alloy had satisfactory impact resistance when used in hammer mills.
- The wear resistance of Ni-Hard 4 Low V alloy under service conditions found in the hammer mill were superior to the standard material and show promise for future applications.

REFERENCES

1. ASM Metals Handbook, Volume 18, Friction, Lubrication and Wear Technology, ASM Desktop Addition, 2001, Edited by Peter J. Blau.
2. "What is Wear Resistant Materials- Definition," Materials Properties.Org, <https://material-properties.org/what-is-wear-resistant-materials-definition/>
3. W.E. Frazier, "Metal Additive Manufacturing: A Review", Journal of Material Engineering, Performance, 2014 Vol. 23, No.6 pp.1917-1928.
4. Standard Specification for Abrasion-resistant Cast Irons, ASTM A532/A532M -10, ASTM, Philadelphia, PA. Reapproved 2019.
5. Properties and Applications of Ni-Hard Alloys, No. 11017, Nickel Institute, Edited by G. Moe, 2021.
6. M.M. Mourad, S. El-Hadad and M.M. Ibrahim, "Effects of Molybdenum Addition on the Microstructure and Mechanical Properties of Ni-Hard White Cast Iron," Transactions Indian Institute of Metals, No.68 Vol. 5. pp. 715-722.
7. M. Mohammadnezhad, V. Javaheri, M. Shamanian, M. Naseri, and M. Bahrami, "Effects of Vanadium Addition on Microstructure," Mechanical Properties and Wear Resistance of Ni-Hard 4 White Cast Iron, Materials and Design, 2013,49, pp.888-893.
8. A. Bedolla-Jacuinde, R. Correa, J.G. Quezada, and C.Maldonado, "Effect of titanium on the as-cast microstructure of a 16% Chromium White Iron," Mater Sci Eng A 2005, 398 pp.297-308.
9. M. Radulovic, M. Fiset, K. Peev, and M. Tomovic, "The influence of vanadium on fracture toughness and abrasion resistance in high chromium white cast irons," J Mater Sci 1994, 29, pp. 5085-5094.
10. R.J. Chung, X.Tang, D.Y. Li, B. Hinckley and K.Dolman, "Effects of titanium addition on microstructure and wear resistance of hypereutectic high chromium cast iron Fe-25 wt%Cr-4 wt%C," Wear 2009;267, pp.356-361.
11. W. Xiaojun, X. Jiandong, F. Hanguang and Z. Xiaohui, "Effect of titanium on the morphology of primary M7C3 carbides in hypereutectic high chromium white iron," Mater Sci Eng A 2007,457, pp.180-185.
12. S.H. Mousavi Anijdan, A. Bahrami, N. Varahram, and P. Davami, "Effects of tungsten on erosion-corrosion behavior of high chromium white cast iron," Mater Sci Eng A 2007, 454, pp. 623-628.
13. Z. Xiaohui, X. Jiandong, F. Hanguang, and X. Bing, "Effect of niobium on the as-cast microstructure of hypereutectic high chromium cast iron," Mater Lett, 2008, 62, pp.857-860.
14. H. Pourasibi and J.D. Gates, "Effects of niobium macro-additions to high chromium white cast iron on microstructure, hardness and abrasive wear behaviour," Materials and Design, Vol. 212, 2021.
15. J.J. Dunkley, "The Factors Determining the Oxygen Content of Water Atomized 304L Stainless Steel Powder," Progress in Powder Metallurgy Edited by J.M Capus and D.L. Dyke, Metal Powder Industries Federation, Princeton, NJ, 1981, Vol. 37, pp. 39-45.
16. F. Bahfie, F. Nuriaman, F.I. Lisa and S. Syafriadi, Effect of Vanadium on the Mechanical Properties and Microstructure of Ni-Hard 2, AIP Conference Proceedings, 2020, 2232.
17. Standard Test Methods for Metal Powders and Powder Metallurgy Products, 2022, Metal Powder Industries Federation, Princeton, NJ.
18. Standard Test Method for Measuring Abrasion Using the Dry Sand/Rubber Wheel Apparatus G65-16, published by ASTM International.
19. K. Horvay, C. Schade, T. Murphy and C. Junghetu, "Microstructure and Mechanical Properties of Wear Resistant Alloys Produced by the Laser Powder Bed Fusion Process," Advances in Additive Manufacturing with Powder Metallurgy, compiled by S. Jones and

M.K. Johnston, Metal Powder Industries Federation, Princeton, NJ., 2023, part 8, pp. 879-891.